

UC Irvine

UC Irvine Previously Published Works

Title

Identification of novel filament-forming proteins in *Saccharomyces cerevisiae* and *Drosophila melanogaster*

Permalink

<https://escholarship.org/uc/item/7dw9b5vg>

Journal

Journal of Cell Biology, 190(4)

ISSN

0021-9525

Authors

Noree, Chalongrat

Sato, Brian K

Broyer, Risa M

et al.

Publication Date

2010-08-23

DOI

10.1083/jcb.201003001

Copyright Information

This work is made available under the terms of a Creative Commons Attribution-NonCommercial-ShareAlike License, available at <https://creativecommons.org/licenses/by-nc-sa/4.0/>

Peer reviewed

Identification of novel filament-forming proteins in *Saccharomyces cerevisiae* and *Drosophila melanogaster*

Chalongrat Noree, Brian K. Sato, Risa M. Broyer, and James E. Wilhelm

Section of Cell and Developmental Biology, University of California, San Diego, La Jolla, CA 92093

The discovery of large supramolecular complexes such as the purinosome suggests that subcellular organization is central to enzyme regulation. A screen of the yeast GFP strain collection to identify proteins that assemble into visible structures identified four novel filament systems comprised of glutamate synthase, guanosine diphosphate-mannose pyrophosphorylase, cytidine triphosphate (CTP) synthase, or subunits of the eIF2/2B translation factor complex. Recruitment of CTP synthase to filaments and foci can be modulated by mutations and regulatory ligands that alter enzyme activity, arguing that

the assembly of these structures is related to control of CTP synthase activity. CTP synthase filaments are evolutionarily conserved and are restricted to axons in neurons. This spatial regulation suggests that these filaments have additional functions separate from the regulation of enzyme activity. The identification of four novel filaments greatly expands the number of known intracellular filament networks and has broad implications for our understanding of how cells organize biochemical activities in the cytoplasm.

Introduction

The principle of self-assembly is believed to underlie the ability of cells to build amazingly complex macromolecular structures such as the mitotic spindle. Most studies of self-assembling structures have focused on either the polymerization properties of cytoskeletal filaments such as actin or microtubules or on the formation of membrane-bound compartments (King and Marsh, 1987; Gardner et al., 2008; Howard and Hyman, 2009; Kueh and Mitchison, 2009). However, the last several years have seen an explosion in the identification of novel intracellular structures such as processing bodies, U bodies, and purinosomes (Sheth and Parker, 2006; Liu and Gall, 2007; An et al., 2008), providing a new arena for identifying the mechanisms that drive the self-assembly of these supramolecular complexes. The identification of these structures has also raised the question of whether this type of organization is an important general mechanism for compartmentalizing the various biochemical reactions that take place in the cytoplasm.

Recently, a partial screen of the yeast GFP collection identified 33 proteins that are capable of self-assembling into large punctate structures that can be isolated biochemically,

arguing that this form of regulation might be quite common (Narayanaswamy et al., 2009). However, it remained unclear whether these structures are evolutionarily conserved, and the role of these structures in regulating the biochemical activity of the enzymes remained an open question. Because a large fraction of the yeast GFP collection remained unexamined, we have conducted a more extensive screen of the yeast GFP strain collection to identify proteins that are capable of assembling into previously undescribed intracellular structures. This screen identified nine proteins that assemble into four distinct cytoplasmic filaments, indicating that the self-assembly of enzymes into large cytoplasmic structures is more common than has been previously believed and that they can form structures other than puncta within the cytoplasm.

We have built on the results of this screen to address the second major question concerning supramolecular complexes: how their assembly is regulated. Allosteric regulation has been thought to control the assembly of enzyme supramolecular

Correspondence to James E. Wilhelm: jwilhelm@ucsd.edu

© 2010 Noree et al. This article is distributed under the terms of an Attribution-Noncommercial-Share Alike-No Mirror Sites license for the first six months after the publication date [see <http://www.rupress.org/terms>]. After six months it is available under a Creative Commons License [Attribution-Noncommercial-Share Alike 3.0 Unported license, as described at <http://creativecommons.org/licenses/by-nc-sa/3.0/>].

complexes such as the purinosome; however, this has never been tested directly (An et al., 2008). To define the relationship between the regulatory state of the enzyme and the formation of filaments/foci, we focused our experiments on the assembly of CTP synthase structures because the regulation of CTP synthase activity has been extensively studied in *Saccharomyces cerevisiae* (Yang et al., 1994; Nadkarni et al., 1995; Ostrander et al., 1998; Pappas et al., 1998). Our experiments revealed that end product inhibition of CTP synthase is necessary for filament assembly, arguing that in CTP synthase, filaments are comprised of an inhibited form of CTP synthase. This suggests that regulation of enzyme activity is central to the assembly of many supramolecular complexes. Furthermore, the discovery of four novel filaments effectively doubles the number of known filament networks present in eukaryotic cells, opening a new area for study with implications for enzyme regulation and cellular organization.

Results and discussion

A visual screen for novel cytoplasmic structures in *S. cerevisiae*

The yeast GFP strain collection is comprised of 4,159 strains of the budding yeast *S. cerevisiae*, which each have GFP fused to the C terminus of a single protein (Huh et al., 2003). However, the original screen of this collection failed to identify several structures, such as P bodies or eisosomes (Sheth and Parker, 2006; Walther et al., 2006). To identify novel intracellular structures, we have visually screened 1,632 GFP-tagged yeast strains comprising 40% of the collection. This screen has identified nine proteins that are capable of forming filaments and foci in vivo and that were reported as having only a cytoplasmic localization in the original characterization of the collection. These proteins are Glt1p (glutamate synthase), Psa1p (GDP-mannose pyrophosphorylase), Ura7p/Ura8p (CTP synthase), Gcd2p (eIF2B- δ), Gcd6p (eIF2B- ϵ), Gcd7p (eIF2B- β), Gcn3p (eIF2B- α), and Sui2p (eIF2- α ; Fig. 1 A). In addition, we identified 29 proteins that were localized to discrete cytoplasmic foci but were not capable of forming filaments (Table I). Although the subcellular localization of Glt1p, Psa1p, and Ura7p has not been previously described, various components of eIF2 and eIF2B have been reported as being present in a novel cytoplasmic body (Campbell et al., 2005). However, the filamentous nature of these eIF2/2B-containing structures was not commented on in those experiments.

One concern with our screen is that the GFP tag might alter the structure or function of the proteins, causing them to form filaments or foci. However, when the GFP tag was replaced with a HA epitope tag, all of the proteins continued to form filaments, arguing that GFP was not responsible for causing these nine proteins to self-assemble (Fig. S1).

As a second assay for the effects of the tag on protein function, we tested whether the GFP-tagged version of each protein exhibited altered growth or viability. Psa1p, Gcd2p (eIF2B- δ), Gcd7p (eIF2B- β), Gcd6p (eIF2B- ϵ), and Sui2p (eIF2- α) are all essential genes, and GFP-tagging each of these genes at the endogenous locus did not affect viability, arguing that the addition of

GFP did not alter the function of these proteins. Ura7p, although nonessential, is one of two genes that encode for CTP synthases in *S. cerevisiae*, and the *ura7 Δ ura8 Δ* double mutant is inviable. We took advantage of this synthetic lethality to examine the effects of the GFP tag on Ura7p function. To do this, we created a *ura8 Δ* deletion in a *URA7::GFP* background. The *URA7::GFP; ura8 Δ* yeast strain was viable, arguing that the GFP tag did not alter the function of the Ura7p. Unlike the other seven filament-associated proteins that we identified, there is no known phenotype associated with deletion of *GLT1*. Consequently, we were unable to assess whether the GFP tag affected Glt1p function. From these experiments, we conclude that the ability to form filaments is not dependent on GFP and that the GFP tag does not affect protein function for eight of the nine filament-forming proteins that we identified.

Ura7p/Ura8p, Psa1p, Glt1p, and eIF2/2B form distinct cytoplasmic filaments

The identification of nine filament-forming proteins raised the question of whether they are all part of the same filament network or whether they represent distinct cytoplasmic structures. To address this issue, we performed pairwise colocalization experiments between Ura7p, Ura8p, Psa1p, Glt1p, and representative subunits of the eIF2 and eIF2B complexes in which one protein was tagged with GFP while the second was tagged with mCherry. Although representative subunits of the eIF2 and eIF2B complexes were present in the same filament, Ura7p, Psa1p, and Glt1p were each present in distinct filaments (Fig. 1 B). Furthermore, Ura7p and Ura8p, which both encode for CTP synthases in *S. cerevisiae*, coassembled into a common filament, arguing that the ability to self-assemble is conserved between these two proteins (Fig. 1 B). Therefore, we have identified four distinct filaments in yeast. Interestingly, although we observed 100% colocalization between the filaments formed by different eIF2/2B subunits, we also found that eIF2/2B subunits form filaments at different frequencies (Table II). This suggests that although all eIF2/2B subunits assemble into a common structure, the association of certain subunits such as GCN3 that are only observed infrequently in filaments may be regulated.

Ura7p, Psa1p, Glt1p, and eIF2/2B filaments are not affected by known regulators of prion biogenesis

All four of the filaments we have identified bear a superficial resemblance to the filaments formed by prions when they are induced de novo (Zhou et al., 2001). This suggested that some or all of the filaments identified in our screen could be regulated by the same factors that control prion formation or that the filaments that we have identified are novel prions. To test this hypothesis, we deleted two genes required for prion formation/maintenance, *RNQ1* and *HSP104*, from strains in which a filament-associated protein had been tagged with GFP (Chernoff et al., 1995; Sondheimer and Lindquist, 2000). The frequency of filament formation for each of the four classes of filaments was unaltered in either *rnq1 Δ* or *hsp104 Δ* strains (Fig. 2 A). Thus, neither Rnq1p nor Hsp104p contributes to the formation of any



Figure 1. **Identification of nine proteins capable of filament formation in *S. cerevisiae*.** (A) Nine filament-forming proteins were identified by visual screening of the *S. cerevisiae* GFP strain collection: Glt1p (glutamate synthase), Psa1p (GDP-mannose pyrophosphorylase), Ura7p (CTP synthase), Ura8p (CTP synthase), Gcd2p (eIF2B- δ), Gcd6p (eIF2B- ϵ), Gcd7p (eIF2B- β), Gcn3p (eIF2B- α), and Sui2p (eIF2- α). (B) The nine proteins that are capable of forming filaments were found to reside in four distinct filaments. All images are of cells grown to saturation except for subunits of the eIF2/2B complex, which were from log-phase cultures. These conditions were chosen because they maximized filament formation for the respective subunits.

Table I. **Proteins that assemble into intracellular structures**

Foci-forming protein	Biological process
Prs4p	5-phosphoribose 1-diphosphate biosynthetic process
Acs1p	Acetate fermentation/acetyl-CoA biosynthetic process/histone acetylation
Glt1p	Ammonia assimilation cycle/glutamate biosynthetic process
Ssd1p	Cell wall organization/chronological cell aging/replicative cell aging
Ura7p	CTP synthesis
Hsp42p	Cytoskeleton organization/response to stress
Rnr4p	Deoxyribonucleotide biosynthetic process
Rnr2p	Deoxyribonucleotide biosynthetic process
Psa1p	GDP-mannose biosynthetic process/protein amino acid glycosylation
Gln1p	Glutamine biosynthetic process/nitrogen compound metabolic process
Dug2p	Glutathione catabolic process
Gly1p	Glycine biosynthetic process/threonine catabolic process
Gsy2p	Glycogen biosynthetic process
Gdb1p	Glycogen catabolic process
Gph1p	Glycogen catabolic process
Hem2p	Heme biosynthetic process
His4p	Histidine biosynthetic process
Hek2p	Intracellular mRNA localization/telomere maintenance via telomere
Rim20p	Invasive growth in response to glucose limitation/protein processing/peptidolysis
Sam1p	Methionine metabolic process/S-adenosylmethionine biosynthetic process
Sam2p	Methionine metabolic process/S-adenosylmethionine biosynthetic process
Hsp104p	Protein folding
Ssa1p	Protein folding
Sse2p	Protein folding
Ssa2p	Protein folding
Sis1p	Protein folding
Rpn9p	Proteasome assembly/ubiquitin-dependent protein catabolic process
Gcd6p	Regulation of translation initiation
Sui2p	Regulation of translation initiation
Gcd2p	Regulation of translation initiation
Gcd7p	Regulation of translation initiation
Gcn3p	Regulation of translation initiation
Sgt2p	Response to heat (glutamine-rich cytoplasmic protein of unknown function)
Thr1p	Threonine metabolic process
YAR009Cp	Transposition, RNA mediated
YLR143Wp	Unknown
YMR253Cp	Unknown

Bolded gene names are those proteins that form filaments in addition to foci.

of the four filament networks that we have identified. Consistent with this interpretation, overexpression of Hsp104p had no effect on Ura7p or Psa1p filaments and only weak effects on

Glt1p filament formation (Fig. 2 B). Thus, the ability of Ura7p, Psa1p, Glt1p, and eIF2/2B to form filaments is not regulated by *HSP104* or *RNQ1*, and they are unlikely to be novel prions.

Table II. **Frequency of filament formation in yeast during log-phase growth and at saturation**

GFP strain	Percentage of cells with filaments during log phase	Percentage of cells with foci during log phase	Percentage of cells with filaments at saturation	Percentage of cells with foci at saturation
	%	%	%	%
<i>URA7</i>	0.00 ± 0.00	3.80 ± 1.35	15.20 ± 2.35	5.60 ± 0.38
<i>URA8</i>	0.00 ± 0.00	0.00 ± 0.00	16.40 ± 1.80	3.60 ± 0.74
<i>PSA1</i>	0.00 ± 0.00	0.40 ± 0.08	7.80 ± 0.67	4.80 ± 1.17
<i>GLT1</i>	26.80 ± 3.69	10.40 ± 1.38	39.20 ± 2.05	6.40 ± 1.95
<i>SUI2</i>	66.20 ± 0.87	6.00 ± 0.63	34.60 ± 3.36	5.20 ± 1.17
<i>GCD2</i>	58.40 ± 2.17	9.00 ± 0.37	18.60 ± 2.88	3.60 ± 0.97
<i>GCD6</i>	11.00 ± 0.60	6.40 ± 1.04	18.80 ± 0.98	7.20 ± 1.36
<i>GCD7</i>	37.60 ± 4.52	24.00 ± 4.63	21.00 ± 1.54	19.80 ± 2.17
<i>GCN3</i>	2.80 ± 0.75	0.00 ± 0.00	12.20 ± 0.59	2.80 ± 0.98

Identification of environmental conditions that regulate filament formation

The effects of nutrient deprivation on filament formation. Nutrient deprivation is known to induce the assembly of several cytoplasmic structures such as the processing body (Teixeira and Parker, 2007). To test the role of nutrient deprivation on the assembly of Psa1p, Glt1p, Ura7p, and eIF2/2B filaments, we compared the number of filaments present in log-phase cells with cells grown to saturation ($OD_{600} > 5.0$). Although the number of eIF2/2B filaments declined in saturated cultures relative to log-phase cultures, the number of Glt1p filaments remained fairly constant, whereas Ura7p and Psa1p filaments were significantly increased in saturated cultures (Table II). Each protein also formed foci to varying degrees, with the formation of foci typically being coordinately regulated with filament formation (*URA7*, *URA8*, *PSA1*, *GCD2*, and *GCN3*) or unchanged between log phase and saturation (*GLT1*, *SUI2*, *GCD6*, and *GCD7*; Table II).

One simple explanation for the changes in frequency of filament/foci formation under different growth conditions is that the ability to form these structures merely reflects different protein levels in log phase or saturation. To test this possibility, we measured GFP levels in each of our filament-forming strains in either growth phase through flow cytometry. In general, protein level varied little between log-phase growth and saturation despite dramatic changes in filament formation for these two growth conditions (Fig. S2). Thus, increases in filament/foci formation are not caused by increases in protein expression.

Effects of carbon source depletion on filament formation. Because growth to saturation is a potent inducer of both Ura7p and Psa1p filament formation, we next examined whether media from saturated cultures was capable of inducing filament formation in cultures undergoing log-phase growth. Exposure to YPD (2% peptone, 1% yeast extract, and 2% dextrose) from saturated cultures caused a 4.87-fold increase in the number of cells with Ura7p filaments but had no effect on Psa1p, Glt1p, Sui2p, or Gcd2p filament formation (Fig. 2 C). This result argues that either the depletion of a critical nutrient or the accumulation of a metabolite in the media as cultures approached saturation was responsible for inducing Ura7p filament formation. Furthermore, these results also argue that the mechanism for inducing Psa1p filaments is distinct from that used to promote Ura7p filament formation, even though both filaments are strongly induced in yeast grown to saturation.

Because carbon source depletion is a characteristic feature of saturated cultures that is known to induce other structures such as the processing body (Teixeira et al., 2005), we tested the ability of YP without glucose, water, and water with glucose to induce filament formation in log-phase cultures. Although none of these treatments had a significant effect on Psa1p, Glt1p, Sui2p, or Gcd2p filament formation, treatment with either YP without glucose or water strongly induced Ura7p filament formation (Fig. 2 C). Furthermore, treatment of log-phase cultures with water containing glucose did not induce Ura7p filament formation (Fig. 2 B). Thus, glucose depletion is a potent inducer of Ura7p filament formation and is likely responsible for Ura7p filament formation as cells reach saturation.

These results raised the question of whether filament formation could be reversed by transferring yeast grown to saturation into fresh YPD. The shift to rich media caused no change in the number of Psa1p, eIF2/2B, or Glt1p filaments within 15 min of the shift, whereas the number of Ura7p filaments was decreased 50-fold (Fig. 2 D). Furthermore, when the media shift experiment was conducted with YP lacking glucose, the number of Ura7p filaments only decreased by 1.4-fold, arguing that reversal of filament formation was also strongly dependent on the presence of glucose in the media (Fig. 2 D). Together, these results argue that the presence of glucose in the growth media is a central regulator of Ura7p filament formation and that Ura7p filaments can undergo rapid assembly and disassembly in response to changes in nutrient conditions.

Effect of sodium azide on filament formation. These results suggested that the energy status of the yeast cell rather than the presence or absence of a particular metabolic intermediate in the cell was a critical factor in regulating filament formation. To test this hypothesis, we assayed the effects of treating yeast cells with azide for 15 min to determine whether altering the energy status of the cell without altering the carbon source could also regulate filament formation. Although Ura7p and Psa1p filaments were strongly induced by treatment with sodium azide, the number of Glt1p or eIF2/2B filaments remained unaltered (Fig. 2 E). These results argue that Ura7p and Psa1p filament formation is strongly influenced by the energy status of the cell, whereas Glt1p and eIF2/2B regulation is dependent on other factors.

Effect of protein synthesis inhibitors on filament formation. Because the ability of eIF2/2B to assemble into cytoplasmic bodies had been previously shown to be highly sensitive to treatment with cycloheximide (Campbell et al., 2005), we examined the ability of 100 $\mu\text{g/ml}$ cycloheximide to affect Ura7p, Psa1p, and Glt1p filament formation. For all three of these filaments, treatment with 100 $\mu\text{g/ml}$ cycloheximide for 15 min had no effect on the number of cells possessing filaments, again highlighting the differences in filament regulation (Fig. 2 F).

Effect of temperature on filament formation. Many cytoskeletal filaments such as microtubules depolymerize at low temperatures. To test the role of temperature in filament formation, we shifted both log-phase and saturated yeast cultures to low temperatures for 15 min to determine whether acute changes in temperature would change the proportion of cells possessing filaments. We tested Ura7p, Psa1p, Glt1p, and eIF2/2B filament formation at 0°C. For all of the filaments, we did not detect any change in the frequency of filament formation for either log-phase or saturated cultures at low temperature (Fig. 2 G). Thus, none of the filaments we have identified exhibit the cold-sensitive polymerization characteristic of many cytoskeletal proteins.

Effects of the kinase inhibitor staurosporine on filament formation. Because the assembly of some intermediate filaments is regulated by phosphorylation, we tested whether the kinase inhibitor staurosporine could alter the frequency of filament formation. Exposure of cells to media containing 50 $\mu\text{g/ml}$ staurosporine had no effect on the frequency of Glt1p or eIF2/2B filaments in either log-phase yeast or yeast grown to saturation (Fig. 2 H). However, staurosporine caused a dramatic effect on the number of cells that had either Ura7p

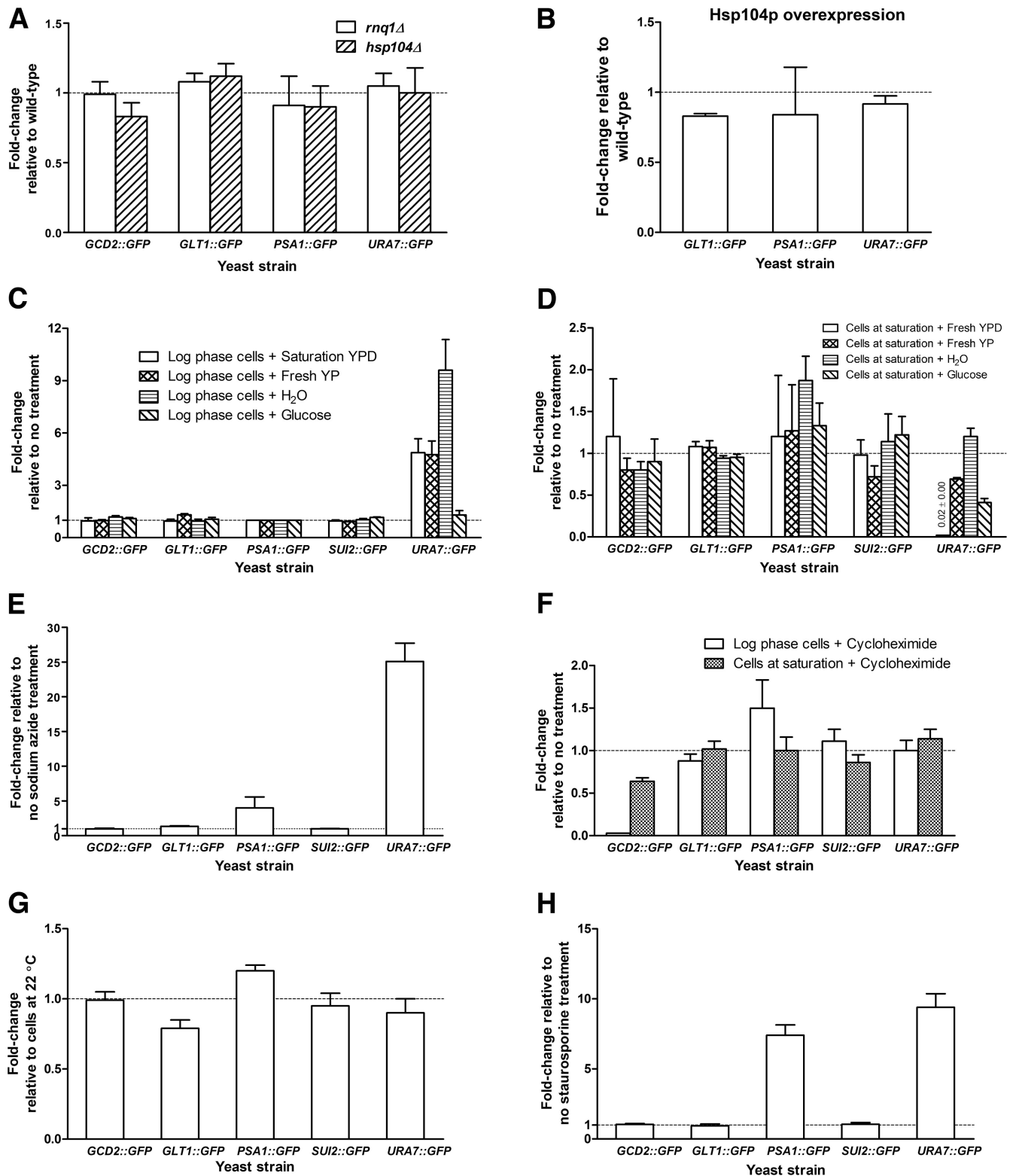


Figure 2. **Regulation of filament formation.** (A) Filament formation is not dependent on either *HSP104* or *RNQ1*. (B) Overexpression of Hsp104p does not affect the formation of Glt1p, Psa1p, or Ura7p filaments. (C) Media lacking glucose strongly induces Ura7p filaments. (D) The addition of media containing glucose triggers disassembly of Ura7p filaments. (E) Treatment with sodium azide causes an increase in Psa1p and Ura7p filaments. (F) Treatment with the translation inhibitor cycloheximide decreases the number of Gcd2p filaments. (G) Exposure of cells to 4°C has no effect on filament formation. (H) Treatment with the kinase inhibitor staurosporine increases Psa1p and Ura7p filaments. (A–H) Error bars represent standard error of the mean. Dashed lines mark the position on the graph where there is no change relative to the reference condition.

or Psa1p filaments, and this effect occurred in both log-phase and saturated yeast cultures (Fig. 2 H). Although further experiments will be necessary to determine whether the effect of staurosporine on Ura7p and Psa1p filaments is direct, the fact that neither Glt1p nor eIF2/2B filaments are affected by the same treatment argues that the effects are not caused by a nonspecific disruption of cellular function.

CTP synthase filament formation is evolutionarily conserved from *S. cerevisiae* to *Drosophila melanogaster*

Given the large number of filaments that we have identified and the fact that they are often regulated by different environmental conditions, we focused our subsequent experiments on one type of filament to determine whether these structures are evolutionarily conserved and to define whether enzyme activity is linked to filament formation. Ura7p filaments provided an excellent starting point for these experiments because CTP synthase is evolutionarily conserved and its enzymology has been extensively characterized. Because a previous study of mammalian CTP synthase found that it colocalized with microtubules, we first tested whether Ura7p was associated with microtubules in yeast (Higgins et al., 2008). Immunostaining for both Ura7p and microtubules showed no colocalization between these structures, arguing that Ura7p filaments are distinct from microtubules (Fig. S3).

We next examined whether the ability of CTP synthase to form filaments was conserved in other species. For these experiments, we took advantage of the fact that the CTP synthase in *Drosophila* had been tagged with GFP at its endogenous locus as part of a genome-wide protein trap screen (Buszczak et al., 2007). Analysis of GFP-CTP synthase in the *Drosophila* egg chamber revealed that filaments formed in all three of the cell types that make up the egg chamber: the nurse cells, the oocyte, and the somatic follicle cells. In nurse cells, two distinct types of filaments were seen: a network of small filaments near the plasma membrane as well as a single large filament that was present in each nurse cell (Fig. 3 A). To confirm the results of the GFP-CTP synthase protein trap, we generated polyclonal antibodies against *Drosophila* CTP synthase. Immunostaining using CTP synthase antibodies confirmed that endogenous CTP synthase assembles into filaments in the three cell types that comprise the egg chamber (Fig. 3 B).

Although CTP synthase is present in all of the cell types of the egg chamber, it remained an open question as to whether all cells and tissues possessed CTP synthase filaments. We approached this question by examining the distribution of CTP synthase filaments in the adult *Drosophila* gut. Our staining revealed that CTP synthase forms filaments in a subset of cells in the gut that are proximal to the gut stem cell (Fig. 3 C). Thus, CTP synthase does not form filaments in every cell within a given tissue in *Drosophila*. Together, these results argue that CTP synthase filament formation is highly regulated in different cell types and tissues.

CTP synthase filament formation is restricted to axons in hippocampal neurons

Because the spatial regulation of cytoskeletal filaments is a common feature of highly polarized cells, we next examined

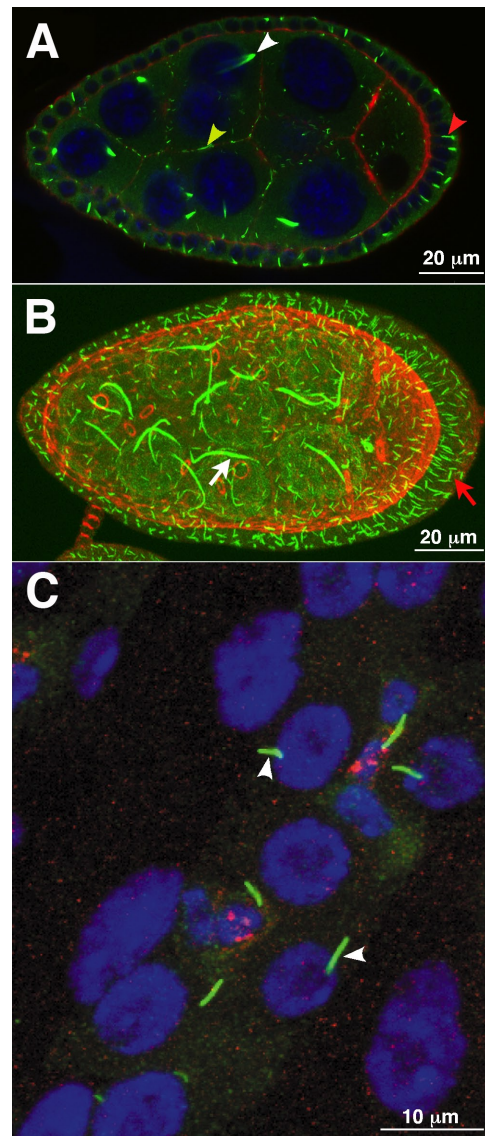


Figure 3. Filament formation is evolutionarily conserved. (A) A single confocal section of a *Drosophila* egg chamber. GFP-CTP synthase (green) is present in small filaments (yellow arrowhead) along the plasma membrane and in large filaments in both the somatic follicle cells (red arrowhead) and nurse cells (white arrowhead). Actin is red, and DNA is blue. (B) A projection of multiple confocal sections of an egg chamber stained with anti-CTP synthase antibody. Large filaments are present in the germline (white arrow) as well as in the somatic follicle cells (red arrow). Actin is red, and CTP synthase is green. (C) In the adult *Drosophila* gut, GFP-CTP synthase (green) labels filaments (arrowheads) in cells clustered near the presumptive gut stem cell, labeled with Delta (red). DNA is blue.

the question of whether CTP synthase filaments could be restricted to particular subcellular domains. To test this possibility, we used immunofluorescence to determine the distribution of CTP synthase filaments in rat hippocampal neurons. These experiments revealed that CTP synthase filaments/foci are restricted to axons and do not occur in dendrites (Fig. 4). Thus, the ability of CTP synthase to form filaments is spatially controlled within neurons, and these filaments represent a novel axon-specific structure.

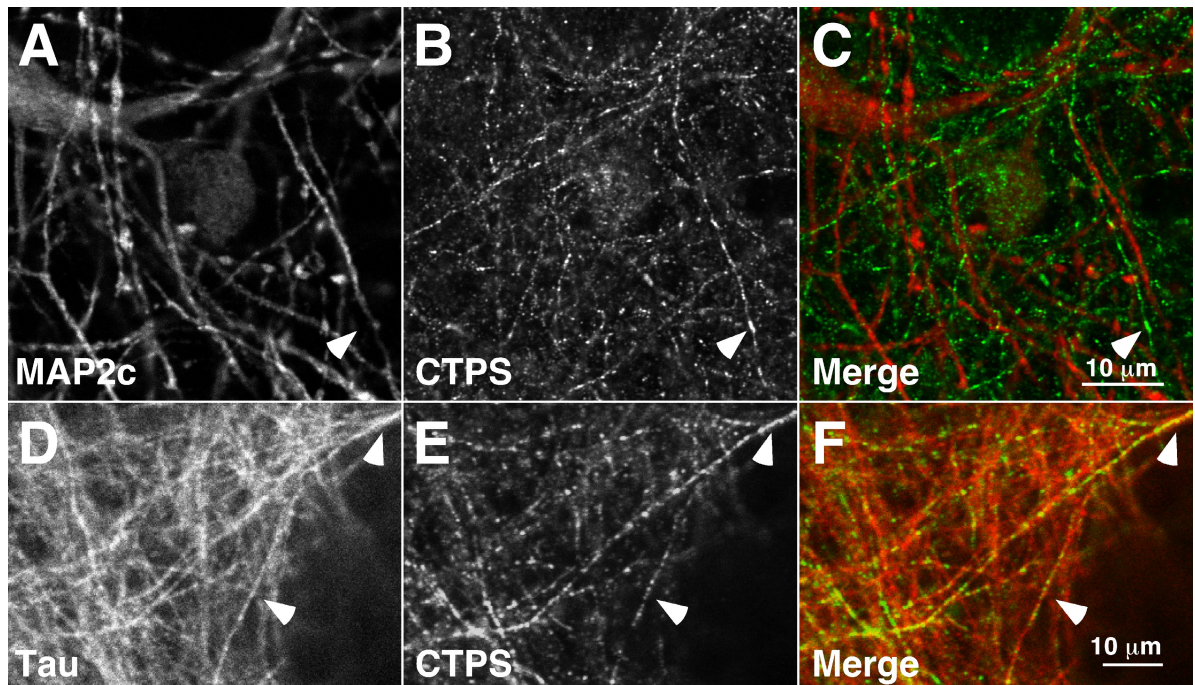


Figure 4. **CTP synthase self-assembles in axons but not in dendrites.** CTP synthase (CTPS) filaments are present in axons (arrowheads) but not dendrites. CTP synthase does not form filaments or foci in dendritic processes. (A–C) MAP2c (A), CTP synthase (B), and a merge (C) are shown. MAP2c is red, and CTP synthase is green. CTP synthase forms filaments and foci in axons (arrowheads). (D–F) Tau (D), CTP synthase (E), and a merge (F) are shown. Tau is red, and CTP synthase is green.

Mutations in *URA7* that prevent feedback inhibition also block filament formation

Self-assembly of enzymes into large cytoplasmic structures has been hypothesized to play several roles ranging from facilitating biosynthetic pathways to storage of inactive enzymes (Sheth and Parker, 2003; Teixeira et al., 2005; An et al., 2008). However, very little is known about how enzyme activity is coupled to the assembly or disassembly of these large cytoplasmic structures. We have taken advantage of previous enzymatic studies of Ura7p to address this issue.

URA7 encodes the major CTP synthase in *S. cerevisiae* that catalyzes the ATP-dependent transfer of the amide nitrogen from glutamine to UTP to generate CTP and glutamate (Ozier-Kalogeropoulos et al., 1991, 1994). CTP synthase activity is regulated by all four nucleotides, and this regulation plays an important role in maintaining the balance in the pyrimidine nucleoside triphosphate pools. Although GTP is an allosteric regulator of the glutaminase activity of the enzyme, ATP, CTP, and UTP all promote the conversion of CTP synthase to the active tetramer. Interestingly, although CTP binding promotes conversion to the active tetramer, it is unique in that it also acts as a competitive inhibitor of CTP synthase activity (Long and Pardee, 1967; Aronow and Ullman, 1987; Pappas et al., 1998; Endrizzi et al., 2005). Previous enzymatic experiments of Ura7p identified a mutation, E161K, that decreased end product inhibition by lowering the affinity of the enzyme for CTP (Ostrander et al., 1998). This prior work presented us with a unique reagent for testing whether enzyme activity was linked to the ability to form filaments. We constructed strains that expressed E161K Ura7p-GFP as the only form of *URA7* to examine filament formation when grown to

saturation. E161K Ura7p formed 20-fold fewer filaments than Ura7p, implying that Ura7p filament formation is strongly associated with decreased CTP binding (Fig. 5 A). Interestingly, although the ability to form filaments was virtually eliminated by the E161K mutation, the frequency of foci formation increased 4.51-fold as compared with wild-type Ura7p. This suggests that the E161K mutation specifically blocks the ability of Ura7p foci to form filaments.

If end product inhibition promotes filament formation, one would also predict that increasing CTP levels would promote self-assembly of CTP synthase. To test this hypothesis, we treated log-phase GFP-Ura7p yeast cells with 10 mg/ml CTP for 15 min (Fig. 5 B). Log-phase yeast cells normally have few Ura7p foci; however, brief exposure to CTP triggered Ura7p self-assembly, causing a 4.4-fold increase in foci. The equivalent treatment of GFP-Glt1p yeast caused no change in the number of Glt1p filaments and foci, indicating that the effect of CTP was specific for Ura7p self-assembly. These results together with our mutant analysis strongly argue that CTP binding is a potent regulator of CTP synthase self-assembly.

To determine whether other regulatory ligands could also drive foci assembly, we treated log-phase GFP-Ura7p yeast cells with 10 mg/ml ATP for 15 min (Fig. 5 B). Treatment with ATP caused a threefold increase in CTP synthase structures, whereas treatment with GTP caused no significant change in foci formation (Fig. 5 B). These results suggested that regulatory ligands that cause enzyme tetramerization also cause CTP synthase to assemble into foci. To test this possibility, we treated cells with AMP-PNP (adenosine 5'-[β , γ -imido]triphosphate), a nonhydrolyzable analogue of ATP which has been previously shown to

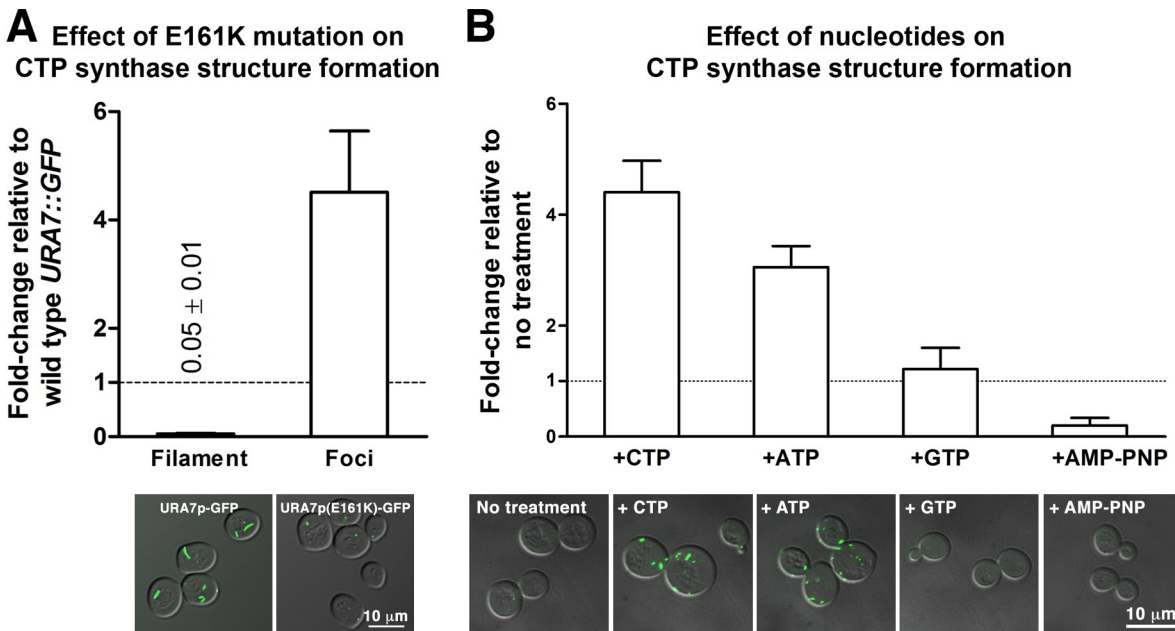


Figure 5. **End product inhibition promotes CTP synthase filament formation.** (A) The E161K mutation causes a 20-fold decrease in Ura7p filament formation. (B) Treatment with CTP and ATP increases Ura7p self-assembly into foci. (A and B) Error bars represent standard error of the mean. Dashed lines mark the position on the graph where there is no change relative to the reference condition.

inhibit Ura7p tetramerization (Pappas et al., 1998). AMP-PNP treatment caused a fivefold decrease in the formation of CTP synthase structures (Fig. 5 B; Pappas et al., 1998). Thus, only regulatory ligands that promote tetramerization are capable of triggering foci formation. These results together with the finding that the E161K mutation blocks filament formation without affecting foci formation suggest that both foci and filament formation by CTP synthase structure are regulated: enzyme tetramerization facilitates foci assembly, whereas end product inhibition is required for filament formation. Future studies directed at the precise regulatory state of the enzyme that allows either filaments or foci to form will help determine whether these two structures are related or whether they represent distinct regulatory states of CTP synthase.

The results of our screen of the yeast GFP strain collection argue that regulated self-assembly of different enzymatic pathways is a common type of biochemical compartmentalization in yeast. Furthermore, we have found that different supramolecular complexes assemble or disassemble in response to distinct environmental conditions. This argues that these different complexes do not form as part of a general stress response but in fact form either to promote or inhibit particular enzymatic processes in response to changing environmental conditions. Additionally, we have found that CTP synthase self-assembly is modulated by the binding of ligands that regulate enzyme activity. This suggests that self-assembly could be a fundamental mode for regulating the enzymes that comprise purinosomes, P bodies, and the additional novel structures that we have identified.

One of the central questions raised by our work in *S. cerevisiae* is whether these structures have additional roles apart from inhibiting or promoting enzyme activity. Clearly, the ability of large cytoplasmic structures to undergo assembly and disassembly in response to changes in the cytoplasmic milieu presents

the cell with a unique sensor that could be used to regulate several cellular processes. Although it is currently unclear whether cells use these structures for such a purpose, the fact that CTP synthase forms filaments in axons and not in dendrites suggests that local regulation of filament formation is possible and may be tied to additional cellular functions. Future work directed at understanding how this spatial regulation is achieved will help identify what additional functions these filaments may serve in neurons as well as in other cell types.

Materials and methods

Yeast strains and media

All yeast strains were derived from a parent strain with the genotype *MATa his3Δ1 leu2Δ0 met15Δ0 ura3Δ0* (S288C). Strains with GFP-tagged genes were from the yeast GFP collection (Howson et al., 2005). All yeast strains were grown at 30°C in YPD unless otherwise indicated. For the testing of various growth conditions, the indicated treatment was applied for 15 min at 22°C unless otherwise noted. For experiments using altered growth media, cells were pelleted, rinsed once with water, and resuspended in the indicated media. Log-phase growth was studied for cells with an OD₆₀₀ under 1.0, and stationary-phase cultures were grown to an OD₆₀₀ of ~5. For Hsp104p overexpression experiments, cells were grown overnight in SD-Leu⁻ (YNB + 2% glucose + 1× Leu dropout amino acid mix) and then diluted into SGR-Leu⁻ medium (YNB + 2% galactose + 1% raffinose + 1× Leu dropout amino acid mix) and grown for 4.5 h. These growth conditions blocked the formation of eIF2/2B filaments, preventing the assessment of the effect of Hsp104p overexpression on filament formation.

Plasmids and DNA methods

For plasmid transformation, genomic tagging of specific loci or gene disruption, the LiOAc method was used (Ito et al., 1983). Genomic tagging and gene disruption were accomplished by transforming yeast strains with a PCR product that encoded G418 resistance and 5' and 3' 50-bp flanks homologous to the gene of interest (Baudin et al., 1993). Cells with the G418 cassette were allowed to grow on YPD for ~24 h and then replica plated onto YPD + 400 μg/ml G418. Gene disruption or genomic tagging was confirmed by PCR. The yeast parent strain was a gift from L. Pillus (University of California, San Diego, La Jolla, CA).

PCR for genomic tagging and gene disruption was performed as follows: KOD hot start polymerase (EMD) was used in 100- μ l reactions (1 \times KOD buffer, 1.25 mM MgSO₄, 200 μ M dNTP, 0.3 μ M of each oligonucleotide, and 100 ng of template). The PCR reaction was performed for 95°C for 2 min, followed by 30 cycles of 95°C for 20 s, 50°C for 10 s, and elongation at 70°C for varying amounts of time. The mCherry-tagging construct (pBS34) was obtained from the University of Washington Yeast Resource Center.

URA7-GFP plasmids were constructed with standard molecular biology techniques. To create the E161K point mutant, the splicing by overlap elongation (SOEing) PCR technique was adapted from Horton et al. (1989). The mCherry-tagging construct (pBS34) was obtained from the University of Washington Yeast Resource Center. The vector used to construct the URA7-GFP plasmids (pRS403) and the construct used for the G418 deletions (pRH728) were gifts from R. Hampton (University of California, San Diego). The Hsp104p overexpression plasmid was a gift of D. Masison (National Institutes of Health, Bethesda, MD; Hung and Masison, 2006).

Antibody generation

The full-length coding region of CG6854-C, the *Drosophila* CTP synthase, was cloned into ProEXHis and expressed as an N-terminal 6 \times His-tagged fusion protein in *Escherichia coli*. Soluble His-CG6854-C was purified using an Ni-nitrilotriacetic acid affinity column, eluted with imidazole, and injected into rabbits (antiserum production by Covance).

Microscopy

Microscopy was performed on a microscope (Axiovert 200M; Carl Zeiss, Inc.) using the software Metavue version 6.3 (MDS Analytical Technologies). Colocalization experiments were performed with a DeltaVision restoration microscopy system (Applied Precision) and microscope (IX70; Olympus) using the software SoftWoRx (Applied Precision).

Flow cytometry

Cells were grown in liquid YPD cultures to the indicated growth phase. Approximately 1 OD of cells was then centrifuged in an Eppendorf tube, rinsed once with water, and resuspended in water. Fluorescence was measured by a Typhoon 9400, and data were analyzed using ImageQuant 5.2 software (GE Healthcare).

Immunofluorescence

For immunofluorescence, yeast cells were removed directly from a selective plate and fixed in 3.7% formaldehyde for 1 h. This was followed by a wash with SK buffer (1 M sorbitol, 45 mM K₂HPO₄, and 7 mM KH₂PO₄) and then a 20-min incubation in SK buffer with 1% β -mercaptoethanol and 10 U zymolyase. Spheroplasts were resuspended in SK buffer and added to slides coated with polylysine (each well treated with 500 μ g/ml polylysine for 10 min, rinsed once with water, and air dried) for 10 min. Samples were fixed in methanol at -20°C for 6 min and then in acetone at -20°C for 2 min. Samples were blocked with 1% BSA in PBS for 20 min, followed by incubation with α -HA antibody (12CA5; Roche) at 4°C overnight. After BSA-PBS washes, samples were incubated with anti-mouse secondary antibody for 2.5 h at room temperature, followed by further washes and mounting of the coverslip. *Drosophila* immunofluorescence was performed as previously described (Wilhelm et al., 2003). This staining used either α -CG6854 antibodies (1:2,000) to stain wild-type ovaries or α -GFP antibody (1:2,000) to stain the GFP protein trap line, CA07332 (M. Buszczak, University of Texas Southwestern Medical School, Dallas, TX), which tags endogenous CG6854 with GFP (Buszczak et al., 2007).

For neuronal staining, neurons dissected from the hippocampus of rat embryos were plated on coverslips and cultured for 14 d using standard conditions (Patrick et al., 2003). Neurons were washed twice in PBS-MC (1 \times PBS, 1 mM MgCl₂, and 0.1 mM CaCl₂) and then fixed in 1 \times PBS, 4% paraformaldehyde, and 4% sucrose for 10 min at room temperature. The coverslips were then washed twice with 1 ml PBS-MC, followed by additional fixation in 1 ml of 100% MeOH (stored at -20°C) for 2 min at -20°C. The coverslips were then washed twice with 1 ml PBS-MC, followed by blocking with 1 ml blocking/permeabilization solution (1 \times PBS-MC with 2% BSA and 0.2% Triton X-100) for 20 min. The blocking solution was then removed, and the coverslips were incubated overnight at 4°C in 1 \times PBS-MC and 2% BSA with primary antibody. The slides were then rinsed three times with PBS-MC, followed by three 5-min PBS-MC washes at room temperature while rotating. The coverslips were then treated with secondary antibody in PBS-MC and 2% BSA for 1 h at room temperature. The secondary antibody was then removed by one 5-min wash in PBS-MC at room temperature while rotating. Slides were then incubated for

10 min in PBS-MC with 2 μ g/ml DAPI, followed by one 5-min wash at room temperature with PBS-MC while rotating. Coverslips were then mounted on slides using Vectashield (Vector Laboratories) and imaged using a laser confocal microscope (TCS SP5; Leica). Primary antibodies were used at the following concentrations: 1:5,000 chicken α -map2c (G. Patrick, University of California, San Diego), 1:100 rabbit α -CG6854 (CTP synthase; bleed no. 110-5), and 1:500 mouse α -tau5 (S. Halpain, University of California, San Diego). Alexa Fluor 488- and Alexa Fluor 568-conjugated α -chick, α -rabbit, and α -mouse secondary antibodies (Invitrogen) were all used at 1:200.

Screening of the yeast GFP collection

Individual strains from the yeast GFP collection were inoculated into 5 ml YPD and cultured overnight at 30°C. The overnight culture was then diluted in YPD to an OD₆₀₀ of ~0.1–0.2 and cultured at 30°C until the OD₆₀₀ = 0.4–0.6. Cells from the original overnight culture and the log-phase culture were pelleted and then washed once with sterile water. The cell pellet was then resuspended in 1.2 M sorbitol and 0.1 M KPO₄ and mounted for imaging with a spinning disk confocal microscope.

Online supplemental material

Fig. S1 demonstrates that filament formation is independent of the GFP tag. Fig. S2 shows an analysis of protein expression level of filament-forming proteins during log-phase growth and saturation. Fig. S3 shows colocalization experiments of Ura7p filaments with microtubules. Online supplemental material is available at <http://www.jcb.org/cgi/content/full/jcb.2011003001/DC1>.

We would like to thank L. Pillus, R. Hampton, G. Patrick, D. Masison, and M. Buszczak for reagents and technical assistance with this project.

C. Noree was supported by the Royal Thai Government Science and Technology Scholarship. B.K. Sato was supported by the University of California, San Diego Faculty Fellows program.

Submitted: 1 March 2010

Accepted: 25 July 2010

References

- An, S., R. Kumar, E.D. Sheets, and S.J. Benkovic. 2008. Reversible compartmentalization of de novo purine biosynthetic complexes in living cells. *Science*. 320:103–106. doi:10.1126/science.1152241
- Aronow, B., and B. Ullman. 1987. In situ regulation of mammalian CTP synthetase by allosteric inhibition. *J. Biol. Chem.* 262:5106–5112.
- Baudin, A., O. Ozier-Kalogeropoulos, A. Denouel, F. Lacroute, and C. Cullin. 1993. A simple and efficient method for direct gene deletion in *Saccharomyces cerevisiae*. *Nucleic Acids Res.* 21:3329–3330. doi:10.1093/nar/21.14.3329
- Buszczak, M., S. Paterno, D. Lighthouse, J. Bachman, J. Planck, S. Owen, A.D. Skora, T.G. Nystul, B. Ohlstein, A. Allen, et al. 2007. The Carnegie protein trap library: a versatile tool for *Drosophila* developmental studies. *Genetics*. 175:1505–1531. doi:10.1534/genetics.106.065961
- Campbell, S.G., N.P. Hoyle, and M.P. Ashe. 2005. Dynamic cycling of eIF2 through a large eIF2B-containing cytoplasmic body: implications for translation control. *J. Cell Biol.* 170:925–934. doi:10.1083/jcb.200503162
- Chernoff, Y.O., S.L. Lindquist, B. Ono, S.G. Inge-Vechtomov, and S.W. Liebman. 1995. Role of the chaperone protein Hsp104 in propagation of the yeast prion-like factor [psi-]. *Science*. 268:880–884. doi:10.1126/science.7754373
- Endrizzi, J.A., H. Kim, P.M. Anderson, and E.P. Baldwin. 2005. Mechanisms of product feedback regulation and drug resistance in cytidine triphosphate synthetases from the structure of a CTP-inhibited complex. *Biochemistry*. 44:13491–13499. doi:10.1021/bi051282o
- Gardner, M.K., A.J. Hunt, H.V. Goodson, and D.J. Odde. 2008. Microtubule assembly dynamics: new insights at the nanoscale. *Curr. Opin. Cell Biol.* 20:64–70. doi:10.1016/j.ceb.2007.12.003
- Higgins, M.J., D. Loisele, T.A. Haystead, and L.M. Graves. 2008. Human cytidine triphosphate synthetase 1 interacting proteins. *Nucleosides Nucleotides Nucleic Acids*. 27:850–857. doi:10.1080/15257770802146502
- Horton, R.M., H.D. Hunt, S.N. Ho, J.K. Pullen, and L.R. Pease. 1989. Engineering hybrid genes without the use of restriction enzymes: gene splicing by overlap extension. *Gene*. 77:61–68. doi:10.1016/0378-1119(89)90359-4
- Howard, J., and A.A. Hyman. 2009. Growth, fluctuation and switching at microtubule plus ends. *Nat. Rev. Mol. Cell Biol.* 10:569–574. doi:10.1038/nrm2713
- Howson, R., W.K. Huh, S. Ghaemmaghami, J.V. Falvo, K. Bower, A. Belle, N. Dephoure, D.D. Wykoff, J.S. Weissman, and E.K. O'Shea. 2005.

- Construction, verification and experimental use of two epitope-tagged collections of budding yeast strains. *Comp. Funct. Genomics*. 6:2–16. doi:10.1002/cfg.449
- Huh, W.K., J.V. Falvo, L.C. Gerke, A.S. Carroll, R.W. Howson, J.S. Weissman, and E.K. O’Shea. 2003. Global analysis of protein localization in budding yeast. *Nature*. 425:686–691. doi:10.1038/nature02026
- Hung, G.C., and D.C. Masison. 2006. N-terminal domain of yeast Hsp104 chaperone is dispensable for thermotolerance and prion propagation but necessary for curing prions by Hsp104 overexpression. *Genetics*. 173:611–620. doi:10.1534/genetics.106.056820
- Ito, H., Y. Fukuda, K. Murata, and A. Kimura. 1983. Transformation of intact yeast cells treated with alkali cations. *J. Bacteriol.* 153:163–168.
- King, M.D., and D. Marsh. 1987. Head group and chain length dependence of phospholipid self-assembly studied by spin-label electron spin resonance. *Biochemistry*. 26:1224–1231. doi:10.1021/bi00379a004
- Kueh, H.Y., and T.J. Mitchison. 2009. Structural plasticity in actin and tubulin polymer dynamics. *Science*. 325:960–963. doi:10.1126/science.1168823
- Liu, J.L., and J.G. Gall. 2007. U bodies are cytoplasmic structures that contain uridine-rich small nuclear ribonucleoproteins and associate with P bodies. *Proc. Natl. Acad. Sci. USA*. 104:11655–11659. doi:10.1073/pnas.0704977104
- Long, C.W., and A.B. Pardee. 1967. Cytidine triphosphate synthetase of *Escherichia coli* B. I. Purification and kinetics. *J. Biol. Chem.* 242:4715–4721.
- Nadkarni, A.K., V.M. McDonough, W.L. Yang, J.E. Stuke, O. Ozier-Kalogeropoulos, and G.M. Carman. 1995. Differential biochemical regulation of the URA7- and URA8-encoded CTP synthetases from *Saccharomyces cerevisiae*. *J. Biol. Chem.* 270:24982–24988. doi:10.1074/jbc.270.42.24982
- Narayanaswamy, R., M. Levy, M. Tsechansky, G.M. Stovall, J.D. O’Connell, J. Mirrielees, A.D. Ellington, and E.M. Marcotte. 2009. Widespread reorganization of metabolic enzymes into reversible assemblies upon nutrient starvation. *Proc. Natl. Acad. Sci. USA*. 106:10147–10152. doi:10.1073/pnas.0812771106
- Ostrander, D.B., D.J. O’Brien, J.A. Gorman, and G.M. Carman. 1998. Effect of CTP synthetase regulation by CTP on phospholipid synthesis in *Saccharomyces cerevisiae*. *J. Biol. Chem.* 273:18992–19001. doi:10.1074/jbc.273.30.18992
- Ozier-Kalogeropoulos, O., F. Fasiolo, M.T. Adeline, J. Collin, and F. Lacroute. 1991. Cloning, sequencing and characterization of the *Saccharomyces cerevisiae* URA7 gene encoding CTP synthetase. *Mol. Gen. Genet.* 231:7–16. doi:10.1007/BF00293815
- Ozier-Kalogeropoulos, O., M.T. Adeline, W.L. Yang, G.M. Carman, and F. Lacroute. 1994. Use of synthetic lethal mutants to clone and characterize a novel CTP synthetase gene in *Saccharomyces cerevisiae*. *Mol. Gen. Genet.* 242:431–439. doi:10.1007/BF00281793
- Pappas, A., W.L. Yang, T.S. Park, and G.M. Carman. 1998. Nucleotide-dependent tetramerization of CTP synthetase from *Saccharomyces cerevisiae*. *J. Biol. Chem.* 273:15954–15960. doi:10.1074/jbc.273.26.15954
- Patrick, G.N., B. Bingol, H.A. Weld, and E.M. Schuman. 2003. Ubiquitin-mediated proteasome activity is required for agonist-induced endocytosis of GluRs. *Curr. Biol.* 13:2073–2081. doi:10.1016/j.cub.2003.10.028
- Sheth, U., and R. Parker. 2003. Decapping and decay of messenger RNA occur in cytoplasmic processing bodies. *Science*. 300:805–808. doi:10.1126/science.1082320
- Sheth, U., and R. Parker. 2006. Targeting of aberrant mRNAs to cytoplasmic processing bodies. *Cell*. 125:1095–1109. doi:10.1016/j.cell.2006.04.037
- Sondheimer, N., and S. Lindquist. 2000. Rnq1: an epigenetic modifier of protein function in yeast. *Mol. Cell*. 5:163–172. doi:10.1016/S1097-2765(00)80412-8
- Teixeira, D., and R. Parker. 2007. Analysis of P-body assembly in *Saccharomyces cerevisiae*. *Mol. Biol. Cell*. 18:2274–2287. doi:10.1091/mbc.E07-03-0199
- Teixeira, D., U. Sheth, M.A. Valencia-Sanchez, M. Brengues, and R. Parker. 2005. Processing bodies require RNA for assembly and contain nontranslating mRNAs. *RNA*. 11:371–382. doi:10.1261/rna.7258505
- Walther, T.C., J.H. Brickner, P.S. Aguilar, S. Bernales, C. Pantoja, and P. Walter. 2006. Eisosomes mark static sites of endocytosis. *Nature*. 439:998–1003. doi:10.1038/nature04472
- Wilhelm, J.E., M. Hilton, Q. Amos, and W.J. Henzel. 2003. Cup is an eIF4E binding protein required for both the translational repression of *oskar* and the recruitment of Barentsz. *J. Cell Biol.* 163:1197–1204. doi:10.1083/jcb.200309088
- Yang, W.L., V.M. McDonough, O. Ozier-Kalogeropoulos, M.T. Adeline, M.T. Flocco, and G.M. Carman. 1994. Purification and characterization of CTP synthetase, the product of the URA7 gene in *Saccharomyces cerevisiae*. *Biochemistry*. 33:10785–10793. doi:10.1021/bi00201a028
- Zhou, P., I.L. Derkatch, and S.W. Liebman. 2001. The relationship between visible intracellular aggregates that appear after overexpression of Sup35 and the yeast prion-like elements [PSI(+)] and [PIN(+)]. *Mol. Microbiol.* 39:37–46. doi:10.1046/j.1365-2958.2001.02224.x